Journal of Advanced Concrete Technology
Materials, Structures and Environment

A Design Proposal for Concrete Cover Separation in Beams Strengthened by Various Externally Bonded Tension Reinforcements

Dawei Zhang, Tamon Ueda, Hitoshi Furuuchi
Journal of Advanced Concrete Technology, volume 10 (2012), pp. 285-300

Scientific paper

A Design Proposal for Concrete Cover Separation in Beams Strengthened by Various Externally Bonded Tension Reinforcements

Dawei Zhang[1], Tamon Ueda[2] and Hitoshi Furuuchi[3]

Received 15 February 2012, accepted 4 September 2012 doi:10.3151/jact.10.285

Abstract:

Previous research has shown that the application of externally bonded reinforcements (steel plates, fiber-reinforced polymer (FRP) laminates, overlays, etc.) to strengthen reinforced concrete (RC) beams can lead to brittle debonding failures before the ultimate load is reached. The aim of this study is to develop an analytical approach for the flexural strengthening of existing structures using various types of external reinforcements and predicting the debonding failure. In this study, an analytical model is developed to predict concrete cover separation failure in beams with overlay strengthening that is also applicable to strengthening using other reinforcements, such as steel plates and FRP laminates. An experimental database with various types of beam specimens is used to verify the model's validity and reliability. A concept for determining the effective strengthening capacity in a strengthening design is presented and the main parameters affecting the strengthening capacity are investigated. Finally, a design proposal is presented for the flexural strengthening of RC beams with respect to concrete cover separation failure. This proposal contributes to the application of external flexural strengthening in practical design.

1. Introduction

Bonding external tension reinforcements to a reinforced concrete (RC) structure is an effective and convenient method to improve the structure's static and fatigue performances under service loads and increase its ultimate strength. Initially, much of the research on this topic focused on bonding steel plates to the concrete members (Hussain *et al*. 1995; Jones *et al*. 1982, 1988; Oehlers 1992; Swamy *et al*. 1987). Subsequently, research on the use of Fiber-Reinforced Plastic (FRP) laminates became more prevalent (Gao *et al*. 2004a,b; Maalejand and Bian 2001; Rahimi and Hutchinson 2001; Fanning and Kelly 2001; Quantrill *et al*. 1996; Garden and Hollaway 1998; garden *et al*. 1997; Arduini *et al*. 1997; Nguyen *et al*. 2001; Ahmed andVan Gemert 1999a,b; Beber *et al*. 1999; Smith and Teng 2002; Oller 2009; Wu *et al*. 2005). Most recently, the literature has focused on the use of overlays (Zhang *et al*. 2009, 2011a,b, 2012; Satoh and Kodama 2005). The overlay method consists of arranging tension reinforcements (such as steel bars or FRP grids) under the lower surface of concrete members. Polymer Cement Mortar (PCM) or High-Performance Fiber-Reinforced Cementitious Composites (HPFRCC) is then sprayed onto the reinforcement. Because of the overlay's weak bond strength with normal cement-based materials, PCM or HPFRCC allows higher levels of bond strength and durability.

Although there have been many in situ applications using externally bonded reinforcements to rehabilitate and retrofit structural elements, their use of reinforcements for this purpose is far from being based on a rational design. The development and competitiveness of these technologies depend on the use of valid design guidelines that are based on sound engineering principles and mechanisms. Previous literature has shown that the application of externally bonded reinforcements to strengthen RC structures can lead to brittle failures when the external reinforcements debond before the ultimate load is reached. Such brittle behavior reduces the full utilization of the bonded reinforcement and reduces the structure's safety and stability. Current attempts to explain the premature debonding mechanism fall into two broad categories: (1) an empirical approach to establish a relationship between debonding and various geometrical parameters or various types of applied force at bonding interface; and (2) an analytical approach to predict the stress concentrations that lead to debonding. Although numerous studies have provided design models and methodologies related to the debonding problems of strengthening, the number of studies that provide a general design proposal for various strengthening techniques that addresses their failure mechanism similarities is much smaller.

In this study, a series of experiments are conducted with the aim of developing an analytical approach for the flexural strengthening of existing structures using various types of external reinforcements and predicting the debonding failure. The main objective of this study is to establish an accurate design approach for predict-

[1]Department of Civil Engineering, College of Civil Engineering and Architecture, Zhejiang University, China.
E-mail: dwzhang@zju.edu.cn
[2]Professor, Lab of Engineering for Maintenance System, Hokkaido University, Japan.
[3]Assistant Professor, Lab of Engineering for Maintenance System, Hokkaido University, Japan.

ing the load carrying capacity of strengthened RC beams that experience concrete cover separation failure near the externally bonded reinforcement's cut-off point with various strengthening methods and materials. First, an analytical model is developed to predict concrete cover separation of an overlay-strengthened beam that is also applicable to those strengthened by steel plates or FRP laminates. An experimental database with various types of beam specimens is used to verify the model's validity and reliability. A concept for determining the effective strengthening capacity for a strengthening design is introduced and the main parameters affecting it are investigated. Finally, a design proposal is presented for the flexural strengthening of RC beams with respect to concrete cover separation failure.

2. Concrete cover separation

Among the premature debonding failure modes, concrete cover separation is often observed (see **Fig. 1**). Previous literatures suggest that despite the different materials or methodologies used to strengthen the beam, two major factors control the concrete cover separation failure of an RC beam strengthened with externally bonded reinforcements. The first factors are the initiation and propagation of the concrete cover separation, which can be divided into two stages: 1) formation of a shear crack at the end of the external reinforcement and 2) propagation of the crack to the tension reinforcement level and horizontal progression along the steel reinforcement level. The second factor is the condition to reach the strengthened beam's peak load after the concrete cover separation, which is either 1) yielding of the tension reinforcement at the shear flexure zone to lead to a reduced beam shear resistance or 2) debonding of the concrete cover along the entire shear span to make the flexural strengthening completely inefficient.

The experimental observations indicate that various strengthening methodologies have similar concrete cover separation failure mechanisms. Therefore, a general and valid design procedure will be used for all flexural strengthening types. Current models used to explain the concrete cover separation of a strengthened beam fall into the following categories: (1) derivation of the elastic stress concentrations at the FRP laminate end, (2) the strengthened beam's shear capacity and (3) the concrete tooth model. However, none of the current models can sufficiently predict the failure loads or failure modes (Gao *et al* 2004a; Smith and Teng 2002; Zhang *et al*. 2012). Recently, Zhang *et al*. (2012) developed an analytical model based on the modified concrete tooth model and verified its accuracy. This study further examines the applicability and reliability of this proposed model for steel plate and FRP laminate strengthening.

2.1 Modified tooth model by Zhang *et al*. (2012)

As shown in **Fig. 2**, a series of cracks in the concrete cover cause concrete blocks to form along the bottom of the RC beam that have slits between them resembling "comb teeth". The concrete tooth model was developed under the assumption that a concrete "tooth" between two adjacent cracks deforms similar to a cantilever with horizontal shear stresses acting on its tip, which results from the external reinforcement's different tension forces (Raoof and Hassanen 2000; Zhang *et al*. 1995). For a single tooth (or concrete block) within a given tooth spacing S_{cr} (as indicated in **Fig. 2**), the external reinforcement's tensile stress σ_s generates the tensile stress σ_A at point A which is right beneath internal reinforcement and the closest to the overlay cut-off point in the tooth. According to the debonding criteria, concrete cover failure occurs when the concrete tensile stress σ_A is greater than the concrete's tensile strength. According to Zhang *et al*. (2012), by assuming that all the teeth within the length L_p ranging from the overlay end to the shear flexure crack (Point C in **Fig. 2**) are assumed to have the same tooth spacing S_{cr} and fail simultaneously, and based on the experimental fact that the peak load is reached after the yielding of tension reinforcement at point C in the substrate beam after debonding, the concrete cover separation failure load for overlay-strengthened beams is determined by the following equation:

$$p_{dy} = \frac{2M_{ru}}{(d_0 + L_p)} \tag{1}$$

where M_{ru} is the bending moment at the tension reinforcement yielding of an unstrengthened (control) beam,

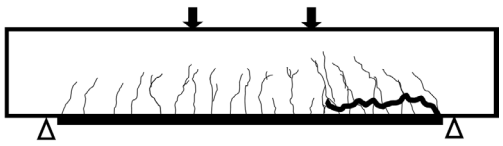

Fig. 1 Concrete cover separation of an RC beam strengthened with externally bonded reinforcement

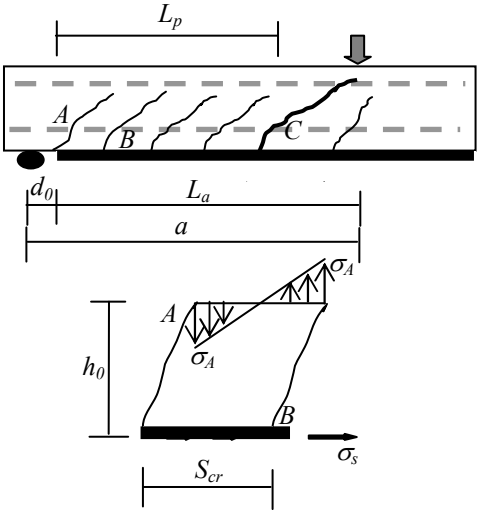

Fig. 2 Concrete tooth model

and L_p is the concrete cover's debonding length at the failure load. L_p can be calculated using the following equation:

$$L_p = \frac{6h_0 A_s (d_s - x_g) M_{ru}}{f_{ct} b S_{cr} I_s} \quad (2)$$

where d_0 is the distance between the support and the end of the overlay; h_0 is the net concrete cover height measured from the bottom side of the substrate concrete's reinforcing bar to the center of the external reinforcement; b is the width of the beam; and A_s is the cross-sectional area of the external reinforcement (either an FRP grid or a steel bar) inside the overlay; x_g, d_s and I_s are the neutral axis depth of the cracked section with strengthening, the effective depth of the external reinforcement and the transformed moment of inertia of the beam's cracked cross-section in terms of the external reinforcement, respectively; and f_{ct} is the substrate concrete's tensile strength.

Based on experimental observations, Zhang *et al*. assume that the average spacing of the concrete teeth (S_{cr}) in Eq. 2 is the same as the average flexure crack spacing (S_{fl}) before the diagonal tension crack is formed and two-thirds of the average flexure crack spacing after the diagonal tension crack is formed, which is the same as the minimum flexural crack spacing. The average flexure crack spacing of an overlay-strengthened beam is given by the following equation:

$$S_{fl} = \frac{3kf_{ct}\left(A_{ct} + A_{ot}\frac{E_o}{E_c}\right)}{\left(\sum O_r \tau_{bcm} + \sum O_s \tau_{bcm}\right)} \quad (3)$$

where k is a coefficient to account for the strain gradient ($k = (\varepsilon_1 + \varepsilon_2)/2\varepsilon_1$, where ε_1 and ε_2 are the largest and smallest tensile strains in the effective embedment zone, respectively); E_o and E_c are the Young's moduli of the overlay material and substrate concrete, respectively; $\sum O_r$ and $\sum O_s$ are the total perimeters of the concrete reinforcement and overlay, respectively; and τ_{bcm} and τ_{bom} are the maximum bond stresses at the reinforcement-concrete interface and the reinforcement-overlay interface at the primary crack formation stage, respectively. These stresses can be calculated using the following equation:

$$\tau_{bc(o)m} = 5.5 \cdot \left(\frac{f'c(o)}{20}\right)^{0.25} \quad (4)$$

where $f'_{c(o)}$ is the compressive strength of the concrete or the overlay material, and A_{ct} and A_{ot} are the effective tension areas of the concrete and the overlay, respectively. According to An *et al*. (1997), for a certain steel bar or FRP grid, the maximum effective tension area of the reinforced concrete (A_{ctmax}) or the overlay (A_{otmax}) within which a stable crack can develop is given by the following equation:

$$A_{c(o)t\max} = \frac{A_{r(s)} \cdot f_{yr(s)}}{f_{c(o)t}} \quad (5)$$

where $A_{r(s)}$ and $f_{yr(s)}$ are the area and the yielding strength of the single tension reinforcement in the concrete (or overlay), respectively, and $f_{c(o)t}$ is the tensile strength of the concrete (or overlay material). When considering two dimensions, the maximum side length of the square effective tension zone for a reinforcing bar in concrete substrate (h_{ctmax}) or overlay (h_{otmax}) can be calculated using the following equation:

$$h_{c(o)t\max} = \sqrt{A_{c(o)\max}} \quad (6)$$

The effective tension zone of a steel bar or an FRP grid should be limited by the cover thickness of the concrete (h_{ctc}) or the overlay (h_{otc}). In bending cases, the height of the effective tension area should not be higher than that of the area in tension ($h_{c(o)tt}$), which is below the neutral axis (shown in **Fig. 3**).

According to ACI Code 318-02 (2002), in regions with large shear forces and small moments, diagonal tension cracks are formed at the following shear force:

$$V_{cd} = 0.31\sqrt{f_c'}\, b_w d_{eff} \quad (7)$$

where d_{eff} is the overlay-strengthened beam's effective depth. Eq. 7 is used to identify diagonal tension crack formations.

2.2 Steel plate and FRP laminate strengthening

The concrete cover separation failure mechanism of steel plate or FRP laminate strengthening is similar to that of overlay strengthening, with differences in the external reinforcement's geometry, material characteristics and bonding agencies. Because this study focuses on concrete cover separation failure rather than failure due to external reinforcement delamination, the effect of the bonding agency on the bond behavior between the substrate concrete and the external reinforcement is ignored. Before concrete cover separation, a composite beam monolithic reaction is assumed. The aim of this study is to determine whether the proposed failure-

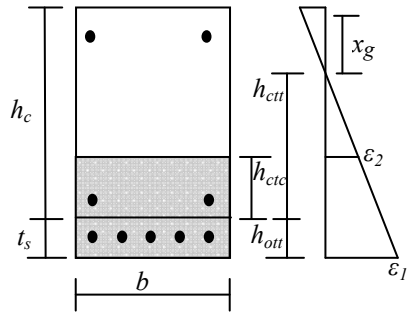

Fig. 3 Effective tension area of an overlay-strengthened beam.

mechanism-based analytical approach for overlay strengthening is applicable to strengthening using steel plates or FRP laminates.

Eqs. 1 and 2 are used to predict the concrete cover separation failure load for a beam strengthened with steel plates or FRP laminates. Special attention is focused on the calculation of average tooth spacing. **Figure 4a** shows a longitudinal segment of the beam strengthened with steel plates or FRP laminates between adjacent cracks subjected to a uniaxial tensile force. The bond stresses at the reinforcement-concrete and the concrete-steel plate (FRP laminate) interfaces at the stabilized crack stage are assumed to follow a parabolic variation according to Kankam (1997) and Jiang *et al*. (1984). **Figure 4b** illustrates a free body diagram of the composite elements with a length of *dx*. Based on the equilibrium of forces acting on the concrete and steel plate (or FRP laminate) segment and the fact that the concrete tensile stress between two adjacent cracks is less than or equal to the concrete tensile strength at the stabilized crack stage, the following equation is derived for the stabilized flexural crack spacing (S_{fl}) of the RC beam strengthened by steel plates or FRP laminates:

$$S_{fl} = \frac{3kf_{ct}A_{ct}}{\left(\sum O_r \tau_{bcm} + b_s \tau_s\right)} \tag{8}$$

where b_s is the width of the FRP laminate or the steel plate and τ_s is the peak bond stress at the FRP laminate (steel plate)-concrete interface at the stabilized crack stage. According to the previous study (Smith and Teng 2002),

$$\tau_s = 1.25 f_{ct} \tag{9}$$

in the FRP laminate case and

$$\tau_s = 0.28\sqrt{f_c'} \tag{10}$$

in the steel plate case. All of the remaining symbols in Eq. 8 are the same as those in Eq. 3. The effective tension area of concrete A_{ct} is calculated based on Eqs. 4 and 5. **Figure 5** shows the comparison of average crack spacing between experimental results ($S_{fl.EXP}$) of 28 and 14 RC beams flexurally strengthened with FRP laminate (Ceroni and Pecce 2009) and with steel plate (Macdonald and Calder 1982) respectively and analytical results from proposed equations ($S_{fl.CAL}$). The mean value and standard deviation of $S_{fl.CAL}/S_{fl.EXP}$ are also presented. The proposed equations can properly predict the average crack spacing of both FRP and steel plate strengthened RC beams.

From these equations, a general calculation flowchart can be composed for identifying the inherent failure mode of RC beams strengthened with various externally bonded reinforcements with respect to concrete cover separation. As indicated in **Fig. 6**, the tooth spacing (S_{cr}) is initially assumed to be the average flexural crack spacing (S_{fl}). If the calculated debonding load (P_{dy}) is

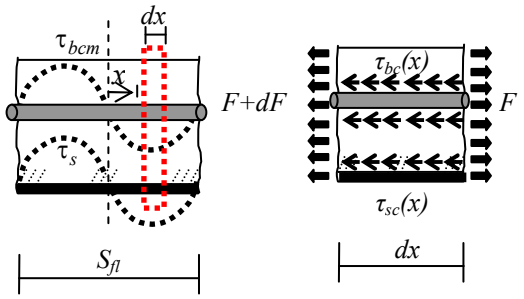

a. Bond stress distribution b. Free body diagram

Fig. 4 Element analysis of composite.

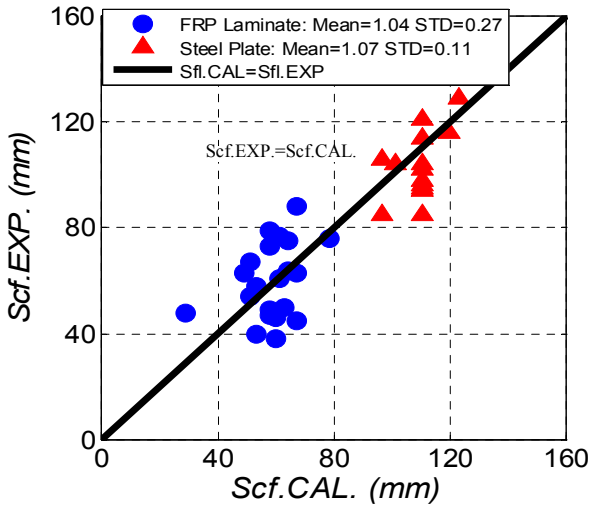

Fig. 5 Comparison between analytical and experimental average crack spacing of FRP strengthened beam.

greater than the diagonal shear cracking load (V_{cd}), the diagonal shear cracks occur before the concrete cover separation, after which the tooth spacing is taken as two-thirds of the average flexural crack spacing following suggestion of Zhang *et al*. (2012), and the debonding load (P_{dy}) has to be recalculated. If the recalculated debonding load is smaller than the diagonal shear-cracking load, concrete cover separation occurs right after the diagonal shear cracks are formed (P_{dy}=V_{cd}). If L_p>a-d_0, the concrete cover fully separates along the shear span, which results in a complete loss of the strengthening capacity. Thus, the peak load depends on the control beam's flexural strength (P_{uc}). The flexure strength (P_{us}) of the strengthened beam without concrete cover separation can be predicted using the conventional analysis approach (JSCE 2007) under the assumption that the external reinforcement and the substrate beam are monolithic. By comparing the debonding strength with the theoretical flexure strength without concrete cover separation, the peak load P_{cal} and the failure mode of a strengthened beam are governed by the lesser of P_{dy} and P_{us}. Please note that this analysis does not consider shear failure of the strengthened beam without debonding.

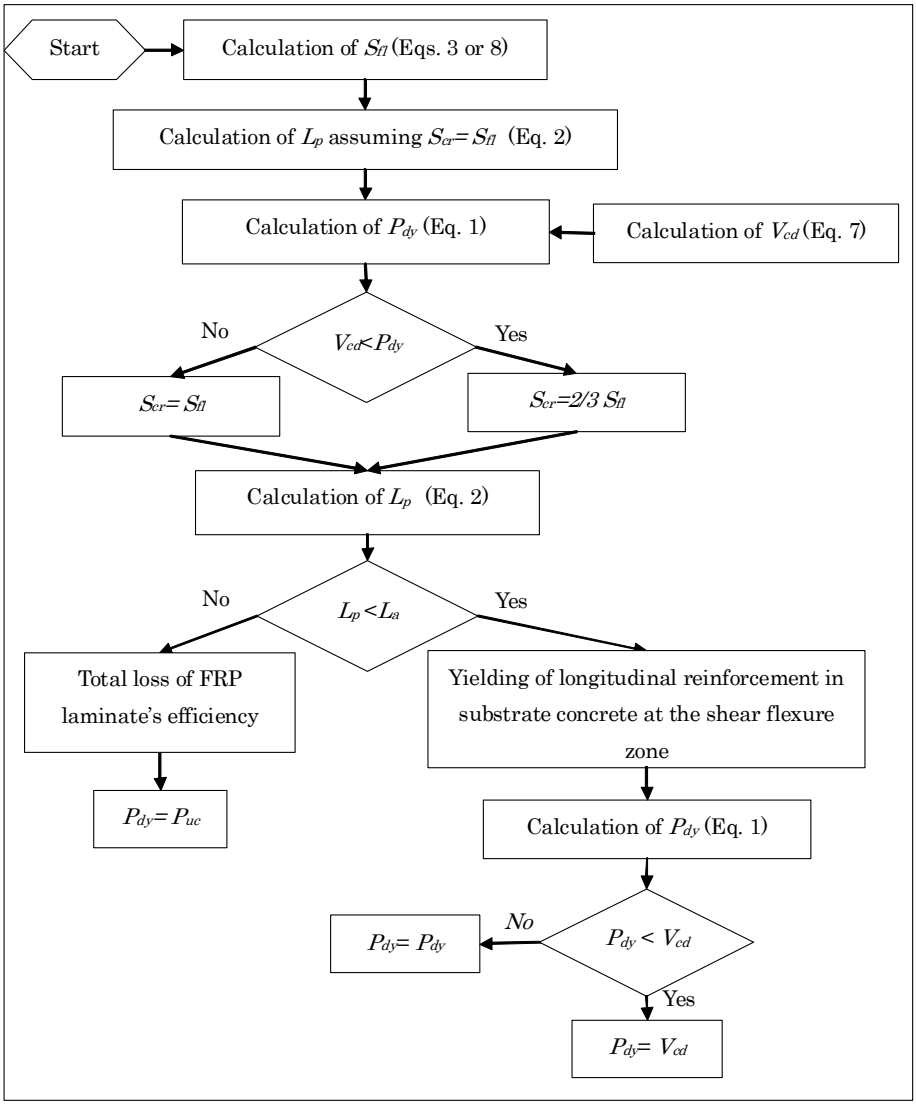

Fig. 6 Calculation flowchart for the flexural-strengthened beam regarding concrete cover separation

2.3 Experimental verifications

To examine the applicability of the proposed models to FRP laminate or steel plate strengthening, the calculated peak and failure loads must be compared with the experimental outputs available in the literature. For this purpose, published or reported experimental results for beams strengthened with FRP laminates or steel plates with sufficient dimensional and material parameters were analyzed. Ninety samples were collected, of which 39 were strengthened with steel plates and 51 were strengthened with FRP laminates. Please note that these samples typically had different material properties and dimensions, including the concrete compressive strength (f'_c), the FRP laminate or steel plate modulus (E_s), the thickness (t_s) and width (b_s) of the FRP laminate or the steel plate, the internal steel reinforcement, the distance from end of the FRP laminate or the steel plate to the support (d_0), and the concrete beam geometry. All of the test data included in this study's database were obtained for simply supported rectangular RC beams subjected to a monotonic four-point bending load, with flexural failure or concrete cover separation. The specimen with interfacial debonding was not considered in this database since it was out of the scope of this paper. The geometrical and material properties of the collected samples are shown in Appendices A and B, respectively.

In **Tables 1** and **2**, each sample's peak load and failure mode are presented, along with numerical estimations based on the proposed model for FRP laminate and steel plate strengthening, respectively. A comparison of the experimental and analytical peak loads is provided in **Fig. 7**. For FRP laminate strengthening, the mean

value of the ratio between the calculated and experimental peak loads (P_{cal}/P_{exp}) is 1.00, with a standard deviation of 0.17 and a correlation coefficient of 0.94. For steel plate strengthening, the mean value of the same ratio is 0.96, with a standard deviation of 0.14 and correlation coefficient of 0.98. The proposed model correctly predicts the effects of various parameters, such as material properties and sample dimensions. These results verify the proposed model's accuracy and indicate that the proposed prediction method is applicable and reliable for FRP laminate and steel plate strengthening as well as overlay strengthening.

3. General design proposal

3.1 Effective (Maximum) Strengthening Capacity

Specimen *Ga1* in **Table 1**, which is strengthened by an external FRP strip, is used as an example to examine the changes of flexural strength and debonding strength with concrete cover separation with area of external reinforcement (A_s). As indicated in **Fig. 8**, for given substrate and external reinforcement material properties, an increase in the ratio of area of external and internal reinforcement A_s/A_r causes the flexural strength to increase and the debonding strength to decrease with concrete cover separation. Therefore, there is an upper limit for the efficient area of external reinforcements, beyond which debonding with concrete separation occurs. In other words, for the given substrate and external reinforcement materials, the strengthening efficiency is limited to a certain range, out of which a further increase in the area of external reinforcement leads to a decrease in the peak load. As shown in **Fig. 8**, the efficient external reinforcement area (A_{eff}) and the effective strengthening capacity (P_{eff}) correlate to the intersection point (P_{dy}=P_{us}) of two curves representing the flexure and debonding strengths, respectively. The strengthened beam experiences flexure failure if $A_s < A_{eff}$ and concrete cover separation failure if $A_s > A_{eff}$. The A_{eff} and P_{eff} for each of the samples were calculated for FRP laminate and steel plate strengthening. Moreover, the overlay-strengthened beams summarized by Zhang *et al*. (2012) were also calculated, of which eight had overlays with steel bars as reinforcements, and 12 had overlays with FRP grids as reinforcements. **Tables 1-4** show the results of these calculations for A_{eff} and A_{eff}/A_s. For almost all of strengthening method types, the experimental and predicted failure modes correspond well when comparing A_s and A_{eff}. There are few exceptions in **Table 1**, which show the predicted failure mode does not agree with the experimental facts. But in all of those exceptional cases the ratio of A_{eff}/A_s is close to 1.0.

3.2 Parameters affecting the effective strengthening capacity

For a given substrate RC beam, the geometrical and material characteristics of the external tension reinforcement are varied to increase the P_{eff} and thus the strengthening efficiency. Therefore, the parameters affecting the A_{eff} and P_{eff} will be investigated. In this study, four parameters including Young's modulus (E_s), tensile strength (f_{ys}), area (A_s) of external reinforcement and the distance between the end of the FRP laminate and the support (d_0) are analyzed, which are the main variances of external strengthening chosen during the design process. Again, specimen *Ga1* in **Table 1** is used as an example to conduct quantitative parametric studies.

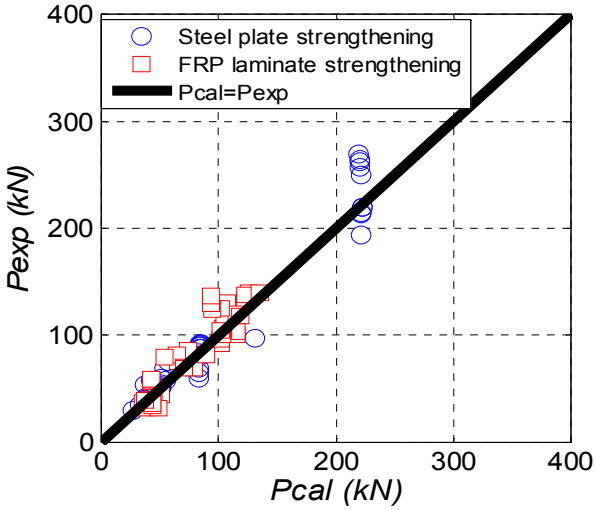

Fig. 7 Comparison between analytical and experimental peak load with concrete cover separation.

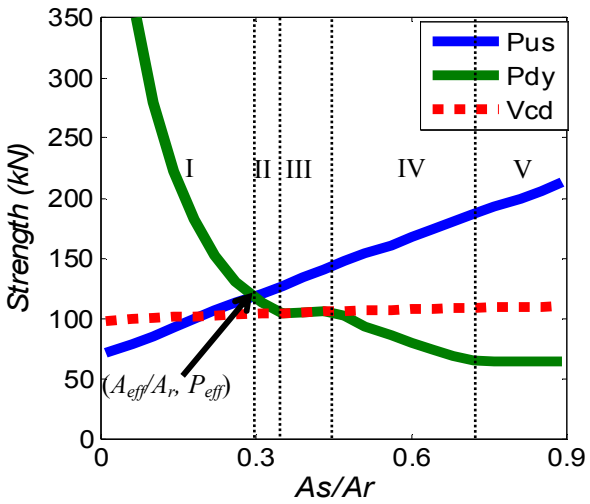

I. $P_{cal}=P_{us}$, $S_{cr}=2/3S_{fl}$, $L_p<L_a$
II. $P_{cal}=P_{dy}>V_{cd}$, $S_{cr}=2/3S_{fl}$, $L_p<L_a$
III. $P_{cal}=P_{dy}=V_{cd}$, $S_{cr}=2/3S_{fl}$, $L_p<L_a$
IV. $P_{cal}=P_{dy}<V_{cd}$, $S_{cr}=S_{fl}$, $L_p<L_a$
V. $P_{cal}=P_{uc}$, $S_{cr}=S_{fl}$, $L_p \geq L_a$

Fig. 8 Effective strengthening capacity.

Table 1 Calculated and experimental results for the RC beam strengthened with FRP laminates.

Name	P_{dy}	P_{uc}	P_{us}	P_{eff}	A_{eff}	$P_{cal}=min(P_{dy}, P_{us})$	P_{exp}	P_{cal}/P_{exp}	P_{eff}/P_{uc}	A_s/A_{eff}	*Failure mode*	
	kN	*kN*	*kN*	*kN*	*kN*	*kN*	*kN*				*Cal.*	*Exp.*
Ga1	101.32	52.14	129.91	113.38	22.50	101.32	92	1.10	2.17	1.47	**c**	**c**
Gb1	74.85	50.40	139.45	92.08	18.00	74.85	76	0.98	1.83	3.67	**c**	**c**
Gb2	65.75	50.40	158.18	92.13	18.00	65.75	75	0.88	1.83	5.50	**c**	**c**
MB3	83.63	53.84	73.63	75.93	29.90	73.63	86	0.86	1.41	0.85	**f**	**c**
MB4	63.95	53.84	79.87	75.95	29.90	63.95	82	0.78	1.41	1.28	**c**	**c**
MB5	53.84	53.84	84.92	75.97	29.90	53.87	79	0.68	1.41	1.71	**c**	**c**
A4	78.78	20.26	82.26	79.31	114.00	78.78	69.7	1.13	3.91	1.05	**c**	**c**
A5	78.78	20.26	82.26	79.31	114.00	78.78	69.6	1.13	3.91	1.05	**c**	**c**
B5	70.51	20.26	96.74	79.40	114.00	70.51	69.7	1.01	3.92	1.58	**c**	**c**
B6	70.51	20.26	96.74	79.40	114.00	70.51	69.6	1.01	3.92	1.58	**c**	**c**
FKF5	115.14	65.50	175.49	133.51	74.40	115.14	100	1.15	2.04	1.94	**c**	**c**
FKF6	115.14	65.50	175.49	133.51	74.40	115.14	103	1.12	2.04	1.94	**c**	**c**
FKF7	101.46	65.50	175.49	118.30	57.60	101.46	97.5	1.04	1.81	2.50	**c**	**c**
FKF10	89.33	65.50	175.49	105.18	43.20	89.33	82	1.09	1.61	3.33	**c**	**c**
B2	42.71	16.41	48.31	46.14	84.80	42.71	34	1.26	2.81	1.13	**c**	**c**
B4	46.28	16.41	48.43	47.52	91.20	46.28	35	1.32	2.90	1.05	**c**	**c**
A1c	50.90	17.01	54.34	52.90	89.60	50.90	44	1.16	3.11	1.07	**c**	**c**
A2b	35.71	15.97	43.73	40.74	78.40	35.71	36.7	0.97	2.55	1.22	**c**	**c**
A2c	35.71	15.97	43.73	40.74	78.40	35.71	37.3	0.96	2.55	1.22	**c**	**c**
1U,1.0m	37.46	16.36	52.62	46.28	38.86	37.46	36.5	1.03	2.83	1.41	**c**	**c**
2U,1.0m	37.46	16.36	52.62	46.28	38.86	37.46	32	1.17	2.83	1.41	**c**	**c**
1Au	40.77	16.57	49.24	44.13	37.80	40.77	39.6	1.03	2.66	1.19	**c**	**c**
1Bu	45.14	16.57	49.63	46.87	41.60	45.14	36.5	1.24	2.83	1.09	**c**	**c**
1Cu	49.88	16.57	49.33	49.33	45.00	49.33	31.9	1.55	2.98	1.00	**c**	**c**
2Au	40.77	14.62	43.44	42.32	43.20	40.77	38.5	1.06	2.89	1.04	**c**	**c**
2Bu	45.14	14.62	43.79	44.60	46.80	43.79	34	1.29	3.05	0.97	**f**	**c**
2Cu	49.88	14.62	43.53	46.87	50.40	43.53	35.5	1.23	3.21	0.89	**f**	**c**
3Au	40.77	12.43	36.93	38.82	48.60	36.93	39	0.95	3.12	0.93	**f**	**c**
A3	104.04	70.39	175.74	126.53	69.00	104.04	106	0.98	1.80	2.83	**c**	**c**
A4	104.04	70.39	175.74	126.53	69.00	104.04	104	1.00	1.80	2.83	**c**	**c**
A950	42.79	42.79	82.45	54.76	14.40	42.43	56.2	0.75	1.28	6.67	**c**	**c**
A1100	42.79	42.79	82.45	58.60	20.80	42.43	57.3	0.74	1.37	4.62	**c**	**c**
A1150	42.79	42.79	82.45	59.46	22.40	42.43	58.9	0.72	1.39	4.29	**c**	**c**
NB2	111.05	111.05	136.86	122.89	24.00	107.32	130.1	0.82	1.11	4.00	**c**	**c**
1T6LN	105.36	52.68	201.61	131.66	33.00	105.36	116.2	0.91	2.50	3.00	**c**	**c**
2T6LN	125.41	54.19	231.15	148.50	39.00	125.41	135.9	0.92	2.74	2.54	**c**	**c**
2T6L1a	125.41	54.19	231.15	148.50	39.00	125.41	139.6	0.90	2.74	2.54	**c**	**c**
2T4LN	122.92	54.19	198.66	148.44	39.00	122.92	133.3	0.92	2.74	1.69	**c**	**c**
2T4L1a	122.92	54.19	198.66	148.44	39.00	122.92	137.7	0.89	2.74	1.69	**c**	**c**
DF3	115.84	63.70	154.10	139.97	28.50	115.84	120	0.97	2.20	1.32	**c**	**c**
DF4	102.28	63.70	169.66	136.11	27.00	102.28	125.6	0.81	2.14	1.86	**c**	**c**
AF3	101.44	44.31	112.46	105.64	22.50	101.44	96.6	1.05	2.38	1.11	**c**	**c**
VR5	103.15	45.60	107.90	106.37	50.40	103.15	102.2	1.01	2.33	1.05	**c**	**c**
VR6	103.15	45.60	107.90	106.37	50.40	103.15	100.6	1.03	2.33	1.05	**c**	**c**
VR7	94.94	45.60	127.92	106.45	50.40	94.94	124.2	0.76	2.33	1.83	**c**	**c**
VR8	94.94	45.60	127.92	106.45	50.40	94.94	124	0.77	2.33	1.83	**c**	**c**
VR9	93.03	45.60	145.20	106.53	50.40	93.03	129.6	0.72	2.34	2.62	**c**	**c**
VR10	93.03	45.60	145.20	106.53	50.40	93.03	137	0.68	2.34	2.62	**c**	**c**
CF2-1	101.44	44.31	112.46	105.64	22.50	101.44	104.8	0.97	2.38	1.11	**c**	**c**
CF4-1	140.59	68.03	135.04	136.21	25.50	135.04	140.2	0.96	2.00	0.98	**f**	**c**

f: Flexural failure; **c**: Concrete cover separation

Table 2 Calculated and experimental results of the RC beam strengthened with steel plates.

Name	P_{dy}	P_{uc}	P_{us}	P_{eff}	A_{eff}	$P_{cal}=min(P_{dy}, P_{us})$	P_{exp}	P_{cal}/P_{exp}	P_{eff}/P_{uc}	A_s/A_{eff}	*Failure mode*	
	kN	*kN*	*kN*	*kN*	*kN*	*kN*	*kN*				*Cal.*	*Exp.*
FRB2	66.08	36.97	53.94	59.97	136	53.94	69.6	0.78	1.62	0.74	**f**	**f**
FRB3	56.98	36.97	62.35	59.69	134	56.98	75	0.76	1.61	1.12	**c**	**c**
FRB5	50.64	36.97	70.68	59.40	132	50.64	60	0.84	1.61	1.52	**c**	**c**
FRB7	42.92	36.97	87.03	59.15	130	42.92	58	0.74	1.6	2.31	**c**	**c**
URB2	72.88	27.98	37.32	60.60	432	37.32	40	0.93	2.17	0.28	**f**	**f**
URB3	63.09	27.98	50.40	62.00	368	50.40	55	0.92	2.22	0.65	**f**	**f**
URB4	55.10	27.93	58.64	56.65	372.8	55.10	57.6	0.96	2.03	1.07	**c**	**c**
URB5	37.86	27.98	104.13	55.66	318.4	37.86	53.2	0.71	1.99	2.51	**c**	**c**
1/2/S	83.51	83.51	171.86	92.84	65	83.51	59.4	1.41	1.11	10.0	**c**	**c**
1/2/N	83.51	83.51	171.86	91.73	57.2	83.51	65	1.28	1.1	11.4	**c**	**c**
1/3/S	83.51	83.51	171.86	89.12	39	83.51	83.2	1.00	1.07	16.7	**c**	**c**
1/3/N	83.51	83.51	171.86	85.76	15.6	83.51	69.2	1.21	1.03	41.7	**c**	**c**
1/4/S	83.51	83.51	171.86	94.32	75.4	83.51	82	1.02	1.13	8.62	**c**	**c**
2/1/N	84.46	84.46	172.77	90.13	39	84.46	88	0.96	1.07	16.7	**c**	**c**
2/1/S	84.46	84.46	172.77	96.89	85.8	84.46	80.2	1.05	1.15	7.58	**c**	**c**
2/2/N	84.46	84.46	172.77	90.13	39	84.46	87.6	0.96	1.07	16.7	**c**	**c**
2/2/S	84.46	84.46	172.77	96.89	85.8	84.46	87.6	0.96	1.15	7.58	**c**	**c**
2/3/N	84.46	84.46	172.77	90.13	39	84.46	89.8	0.94	1.07	16.7	**c**	**c**
2/3/S	84.46	84.46	172.77	96.89	85.8	84.46	90.4	0.93	1.15	7.58	**c**	**c**
2/4/N	84.46	84.46	172.77	90.13	39	84.46	92.2	0.92	1.07	16.7	**c**	**c**
2/4/S	84.46	84.46	172.77	96.89	85.8	84.46	89.8	0.94	1.15	7.58	**c**	**c**
5/1/N	84.82	84.82	173.84	87.86	20.8	84.82	91.8	0.92	1.04	31.3	**c**	**c**
5/1/S	84.82	84.82	173.84	95.04	70.2	84.82	87.8	0.97	1.12	9.26	**c**	**c**
6/1/-	50.74	50.74	104.24	55.95	59.8	50.74	50	1.01	1.1	10.9	**c**	**c**
6/2/-	50.74	50.74	104.24	55.95	59.8	50.74	51	0.99	1.1	10.9	**c**	**c**
6/3/-	41.72	41.72	85.71	45.63	54.6	41.72	42.8	0.97	1.09	11.9	**c**	**c**
6/4/-	38.31	38.31	78.71	43.26	75.4	38.31	42.2	0.91	1.13	8.62	**c**	**c**
7/1/S	33.46	33.46	68.69	37.49	70.2	33.46	35	0.96	1.12	9.26	**c**	**c**
8/2/S	26.89	26.89	56.05	29.41	54.6	26.89	29.6	0.91	1.09	11.9	**c**	**c**
204	219.51	219.51	285.89	243.39	137.5	219.51	270	0.81	1.11	2.73	**c**	**c**
205	221.23	221.23	347.41	241.43	142.5	221.23	213	1.04	1.09	5.26	**c**	**c**
208	220.26	220.26	285.14	242.22	135	220.26	264	0.83	1.1	2.78	**c**	**c**
209	222.06	222.06	346.42	240.57	140	222.06	220	1.01	1.08	5.36	**c**	**c**
210	221.27	221.27	348.05	240.25	135	221.27	215	1.03	1.09	5.56	**c**	**c**
216	220.44	220.44	248.18	242.19	150	220.44	262	0.84	1.1	1.25	**c**	**f**
217	220.53	220.53	285.49	240.40	125	220.53	257	0.86	1.09	3.0	**c**	**c**
218	221.77	221.77	348.46	238.85	127.5	221.77	194	1.14	1.08	5.88	**c**	**c**
219	222.38	222.38	347.21	239.89	130	222.38	220	1.01	1.08	5.77	**c**	**c**
224	221.60	221.60	283.11	241.95	142.5	221.60	250	0.89	1.09	2.63	**c**	**c**

f: Flexural failure; **c**: Concrete cover separation

Table 3 Calculated and experimental results of the RC beam strengthened with overlay and steel bars.

Name	P_{dy}	P_{uc}	P_{us}	P_{eff}	A_{eff}	$P_{cal}=min(P_{dy}, P_{us})$	P_{exp}	P_{cal}/P_{exp}	P_{eff}/P_{uc}	A_s/A_{eff}	Failure mode	
	kN	kN	kN	kN	kN	kN	kN				Cal.	Exp.
R4-2-10	83.57	32.12	63.08	77.27	208.00	63.08	69.40	0.91	2.41	0.69	f	f
R4-3-10	66.24	32.12	78.57	69.49	172.20	66.24	75.90	0.87	2.16	1.24	c	c
N4-3-10	61.69	30.20	76.35	66.22	166.80	61.69	65.31	0.94	2.19	1.28	c	c
N4-3-10	61.69	30.20	76.35	66.22	166.80	61.69	67.67	0.91	2.19	1.28	c	c
N8-3-6	93.46	15.10	25.37	53.62	360.00	25.37	27.50	0.92	3.55	0.26	f	f
N8-3-6	93.46	15.10	25.37	53.62	360.00	25.37	27.20	0.93	3.55	0.26	f	f
N6-3-6	89.93	20.14	34.05	65.81	314.28	34.05	39.47	0.86	3.27	0.30	f	f
N6-3-6	89.93	20.14	34.05	65.81	314.28	34.05	37.90	0.90	3.27	0.30	f	f

f: Flexural failure; **c**: Concrete cover separation

Table 4 Calculated and experimental results of the RC beam strengthened with overlay and FRP grids.

Name	P_{dy}	P_{uc}	P_{us}	P_{eff}	A_{eff}	$P_{cal}=min(P_{dy}, P_{us})$	P_{exp}	P_{cal}/P_{exp}	P_{eff}/P_{uc}	A_s/A_{eff}	Failure mode	
	kN	kN	kN	kN	kN	kN	kN				Cal.	Exp.
1	228.97	68.25	104.56	136.81	127.51	104.56	102.70	1.02	2.00	0.41	f	f
2	191.45	48.99	89.57	126.68	126.46	89.566	109.00	0.82	2.59	0.42	f	f
3	112.80	48.99	118.16	115.85	100.32	112.8	99.50	1.13	2.36	1.05	c	c
4	125.24	68.25	128.71	127.47	102.43	125.24	117.50	1.07	1.87	1.03	c	c
5	187.62	47.70	71.37	114.62	102.42	71.369	81.90	0.87	2.40	0.35	f	f
6	172.49	47.70	72.31	109.67	91.08	72.308	81.90	0.88	2.30	0.40	f	f
7	159.54	47.70	73.25	105.62	81.90	73.248	84.50	0.87	2.21	0.44	f	f
8	174.23	47.70	72.31	110.40	92.16	72.308	83.50	0.87	2.31	0.39	f	f
9	106.88	62.71	119.82	115.45	93.98	106.88	113.20	0.94	1.84	1.12	c	c
10	106.88	62.71	119.82	115.45	93.98	106.88	117.50	0.91	1.84	1.12	c	c
11	106.88	62.71	119.82	115.45	93.98	106.88	120.50	0.89	1.84	1.12	c	c
12	106.88	62.71	119.82	115.45	93.98	106.88	126.20	0.85	1.84	1.12	c	c

f: Flexural failure; **c**: Concrete cover separation

3.2.1 Effects of an external reinforcement's bond width (b_s) and thickness (t_s) for a constant strengthening area (A_s)

Figure 9 and **Table 5** show the effects of different FRP bond width (b_s) and thickness (t_s) combinations for a constant strengthening area. When the strengthening area is held constant, bonds that are narrower and thinner have higher debonding strengths with concrete cover separation, while the flexure strength remains constant. Narrowing and thinning FRP strip leads to increases in both A_{eff} and P_{eff}. According to Eqs. 3 or 8, a smaller external reinforcement bond width results in a smaller bond area between concrete and FRP strip, which increases the average crack spacing (S_{fl}) and in turn decreases L_p (following Eq. 2) and increases the debonding strength (following Eq. 1). This effect is more pronounced if an intersection point exists in zone I of **Fig. 8** and less pronounced when the debonding strength depends on the initiation of a diagonal shear crack (zone III in **Fig. 8**). When the strengthening reinforcement area is kept constant, bonds that are thicker and narrower have the better efficiency. However, reducing the FRP bond width also decreases the FRP-concrete interface bond strength, which increases the possibility of FRP delaminating (Oehlers 1992; Smith and Teng 2002; Oller 2009). Therefore, a comprehen-

Table 5 Effect of b_s (*Ga1*).

Case	b_s	A_{eff}	P_{eff}	P_{eff}/P_{uc}
	mm	mm^2	kN	
1	75.0	22.5	113.38	2.17
2	93.8	20.6	109.98	2.11
3	112.5	20.3	109.27	2.10
4	131.3	18.4	105.66	2.03
5	150.0	18.0	104.91	2.01

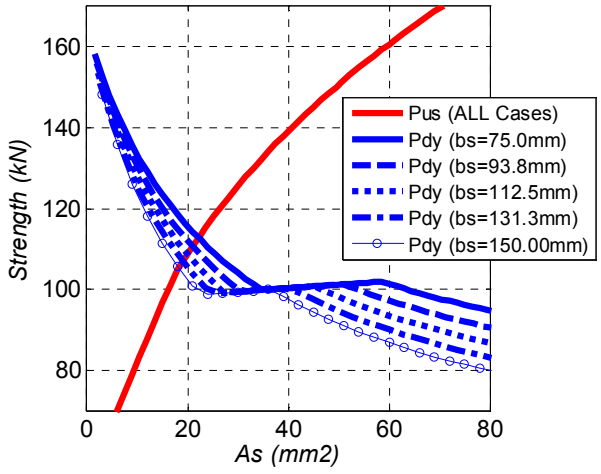

Fig. 9 Effect of b_s (*Ga1*).

sive design should optimize the external reinforcement's width and thickness by considering all debonding mode types.

3.2.2 Effect of d_0

Figure 10 and **Table 6** show the effects of the distance between the end of the FRP laminate and the support (d_0) on the debonding strength and effective strengthening capacity. The debonding strength decreases with increases in d_0, while the flexure strength remains constant. This leads to a reduction in both A_{eff} and P_{eff}. Thus, d_0 should be minimized.

3.2.3 Effect of an external reinforcement's Young's modulus (E_s) for a constant tensile strength (f_{ys})

Figure 11 and **Table 7** show the effect of an external reinforcement's Young's modulus for a constant tensile strength. As E_s increases, the flexure strength increases if the failure is not governed by the tensile strength of external reinforcement and the debonding strength decreases. In this case (as Cases 1 to 3 in **Table 7**), varying E_s only marginally affects P_{eff} and significantly affects A_{eff}. If the flexural strength at the intersection point is governed by the yielding or breakage of external reinforcement, the flexural strength is then not affected by E_s. In this case (as Cases 4 and 5 in **Table 7**), both A_{eff} and P_{eff} decrease with increase of E_s. Generally speaking, smaller E_s is preferable.

3.2.4 Effect of an external reinforcement's tensile strength (f_{ys}) for a constant Young's modulus (E_s)

Figure 12 and **Table 8** show the effect of an external reinforcement's tensile strength of FRP grid or laminate (or yielding strength in case of steel bar or plate) for a constant Young's modulus. As f_{ys} increases, the flexure strength increases if the failure is governed by the yielding or breakage of external reinforcement (as Cases 1 to 3 in **Table 8**), and the debonding strength remains constant. This leads to a decrease in A_{eff} and an increase in P_{eff}. However, if the flexure strength is governed by the compressive failure of concrete before the breakage of external reinforcement (as Case 4 to 5 in **Table 8**), both the flexure strength and debonding strength are constant and consequently A_{eff} and P_{eff} are unchanged. Generally speaking, larger f_{ys} is preferable.

3.3 Calculation of A_{eff} and P_{eff} of all the samples in the database

The effective strengthening capacity was calculated for each of the samples, including those for FRP laminate and steel plate strengthening (collected in this study) and those for overlay strengthening (collected in Zhang *et al.* (2012)). The results of these calculations are shown in **Tables 1-4**. The steel plate strengthening has the lowest strengthening efficiency, with a mean P_{eff} / P_{uc} value of 1.24 (ranging from 1.03 to 2.22). This is

Table 6 Effect of d_0 (*Ga1*).

Case	d_0	A_{eff}	P_{eff}	P_{eff}/P_{uc}
	mm	mm^2	*kN*	
1	60	42.8	142.51	2.73
2	120	27.8	122.12	2.34
3	180	17.2	103.24	1.98
4	240	13.5	92.25	1.77
5	300	8.2	76.73	1.47

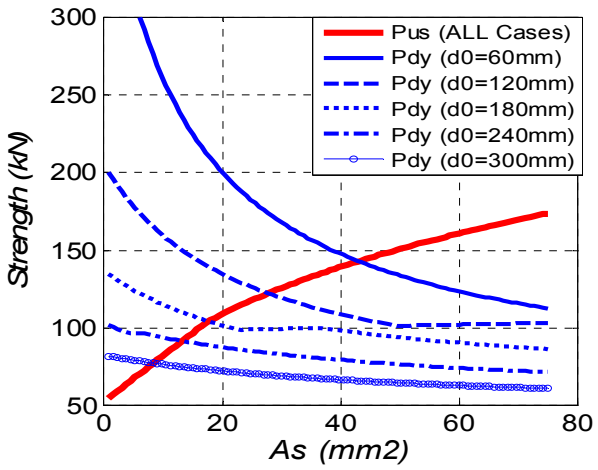

Fig. 10 Effect of d_0 (*Ga1*)

Table 7 Effect of E_s (*Ga1*).

Case	E_s	A_{eff}	P_{eff}	P_{eff}/P_{uc}
	MPa	mm^2	*kN*	
1	7.83E+04	66.0	112.49	2.16
2	1.57E+05	33.0	112.49	2.16
3	2.35E+05	22.5	113.38	2.17
4	3.13E+05	19.5	109.80	2.11
5	3.92E+05	18.0	105.43	2.02

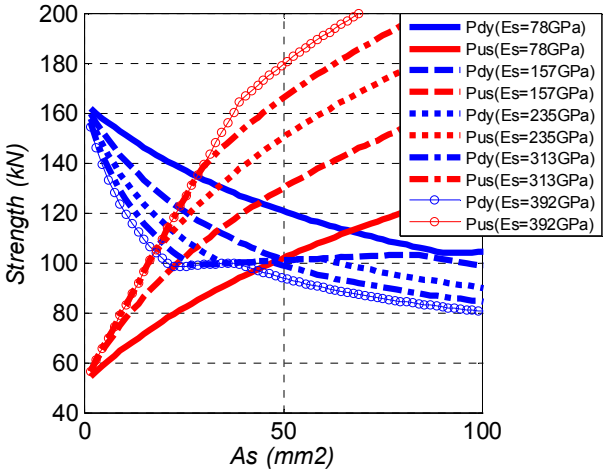

Fig. 11 Effect of E_s (*Ga1*).

mainly due to the relatively low yielding strength of the steel plates, which corresponds well with the parametrical study on f_{ys} in section 3.2.4. Overlay strengthening

Table 8 Effect of f_{ys} (*Ga1*).

Case	f_{ys} *MPa*	A_{eff} mm^2	P_{eff} *kN*	P_{eff}/P_{uc}
1	1050	64.5	99.96	1.92
2	2100	33.0	101.05	1.94
3	3150	25.5	108.71	2.09
4	4200	22.5	113.38	2.17
5	5250	22.5	113.38	2.17

with steel bars and FRP grids as reinforcements and FRP laminate strengthening have relatively higher strengthening efficiencies, with mean P_{eff}/P_{uc} values of 2.82, 2.12 and 2.40, respectively.

3.4 Design proposal

Based on the concept of effective strengthening capacity and its parametric studies, a flow diagram of the strengthening process is proposed (shown in **Fig. 13**). The strengthening of structures typically proceeds in the following steps:

(1) Identify the performance requirements (P_{ep}) for the existing structure to be strengthened.
(2) Inspect the existing structure, evaluate the structure's performance (P_{uc}) and verify whether it fulfills the performance requirements.
(3) If the structure does not fulfill the performance requirements ($P_{uc} < P_{ep}$) and an update of the structure through strengthening is desired, proceed with the structure strengthening design.
(4) Select an appropriate strengthening method and establish the materials (E_s, f_{ys}) and the construction methods (b_s, d_0) to be used.
(5) Evaluate the structure's performance after strengthening (P_{eff}) and verify whether the structure will fulfill the performance requirements.
(6) If the strengthening does not fulfill the performance requirements ($P_{eff} < P_{ep}$), employ the following

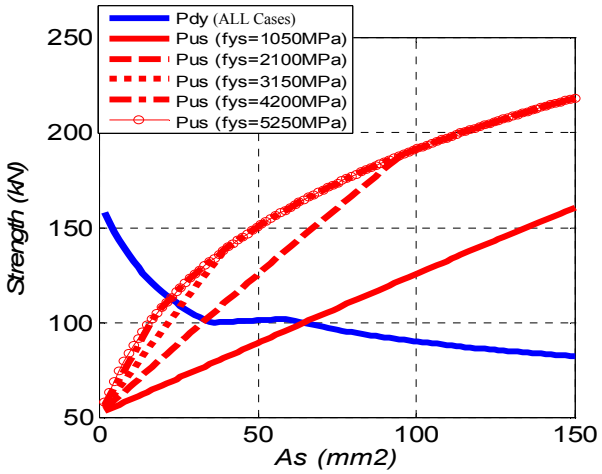

Fig. 12 Effect of f_{ys} (*Ga1*).

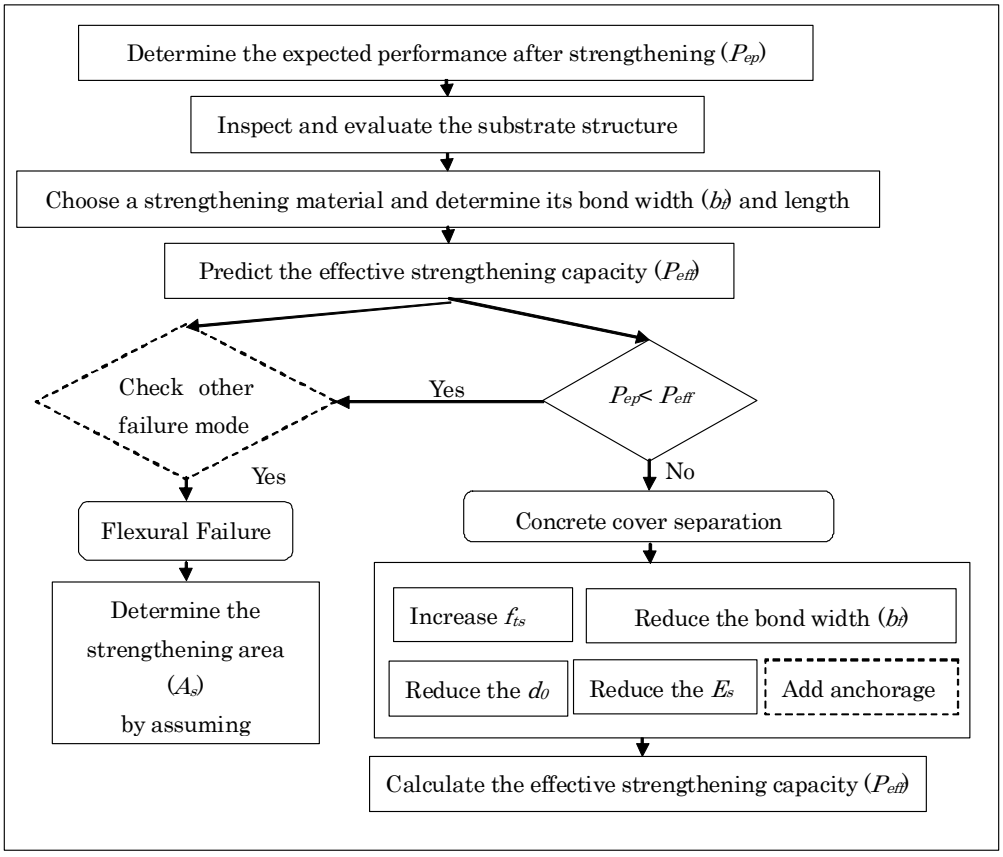

Fig. 13 Design flow chart regarding concrete cover separation

countermeasures and then repeat steps (5) and (6):

a. Reduce the b_s
b. Reduce the d_0
c. Select another material with a lower E_s if E_s governs the flexural strength
d. Select another material with a higher f_{ys} if f_{ys} governs the flexural strength
e. Apply an end anchorage system

(7) If it is determined that the retrofitting structure will fulfill the performance requirements ($P_{eff} \geq P_{ep}$) using the selected strengthening and construction methods, calculate the required strengthening area (A_s) according to P_{ep} under the assumption that the strengthened structure behaves monolithically.
(8) Implement the strengthening work.

4. Conclusions

Bonding external tension reinforcements to a reinforced concrete (RC) structure can significantly improve the ultimate flexural strength and stiffness of the strengthened beams. However, the high ultimate loading capacity is often impaired by premature failure modes, such as concrete cover separation.

In this paper, we have demonstrated that the analytical model developed to predict concrete cover separation in overlay-strengthened beams is also applicable to those strengthened by steel plates or FRP laminates, with differences in the average crack spacing calculations. An experimental database with various types of beam elements was used to verify the model's validity and reliability. For beams strengthened with FRP laminates or steel plates, the proposed model's results correspond well with those from previously conducted experiments.

Based on the analytical model, a concept was presented to determine the efficient strengthening area and effective strengthening capacity by predicting the intersection point of the two curves representing the flexure and debonding strengths. Parametric studies were conducted to clarify the effects of various parameters on the efficient strengthening area and effective strengthening capacity.

Finally, a design flow diagram for the strengthening process was proposed with respect to concrete cover separation. One of the key factors in this diagram is the effective strengthening. This design proposal contributes to the application of external flexural strengthening in practical design.

Acknowledgements

This study is a part of the International Collaborative Research, "Life Cycle Prediction and Management of Concrete Structures" adopted by the Asia-Africa S & T Strategic Cooperation Promotion Program of Special Coordination Funds for Science and Technology of Japan's Ministry of Education, Culture, Sports, Science and Technology. The authors also appreciate the financial aid provided by the Grant-in-Aid for Scientific Research (A) No.22246058.

References

Ahmed, O. and Van Gemert, D., (1999a). "Effect of longitudinal carbon fiber reinforced plastic laminates on shear capacity of reinforced concrete beams." *Proceedings of the fourth international symposium on fiber reinforced polymer reinforcement for reinforced concrete structures.* 933-943.

Ahmed, O. and Van Gemert, D., (1999b). "Behaviour of RC beams strengthened in bending by CFRP laminates." *Proceedings of the eighth international conference on advanced composites for concrete repair.*

American Concrete Institute, (ACI 2002.). "Building code requirements for structural concrete." A*CI 318-02 and Commentary (ACI 318R-02)*, Farmington Hills, Mich..

An, X., Maekawa, K. and Okamura, H., (1997). "Numerical simulation of size effect in shear strength of RC beams." *Journal of Materials, Concrete Structures and Pavements,* 35, 297-316.

Arduini, M., Tommaso, A. D. and Nanni, A., (1997). "Brittle failure in FRP plate and sheet bonded beams." *ACI Structural Journal.* 94(4), 363-70.

Fanning, P. J. and Kelly. O., (2001). "Ultimate response of RC beams strengthened with CFRP plates." *Journal of Composites for Construction*. 5(2), 122-127.

Beber, A. J., Filho, A. C. and Campagnolo, J. L., (1999). "Flexural strengthening of R/C beams with CFRP sheets." *Proceedings of the eighth international conference on advanced composites for concrete repair.*

Ceroni, F. and Pecce, M., (2009). "Design provisions for crack spacing and width in RC elements externally bonded with FRP." *Composites Part B: Engineering,* 40(1), 17-28.

Gao, B., Kim, J. K. and Leung, C. K. Y., (2004a). "Experimental study on RC beams with FRP strips bonded with rubber modified resins." *Composite Science and Technology*, 64, 2557-2564.

Gao, B., Kim, J. K. and Leung, C. K. Y., (2004b). "Taper ended FRP strips bonded to RC beams: Experiments and FEM analysis." *The 2nd international conference on FRP composites in civil engineering,* 399- 405.

Garden, H. N. and Hollaway, L. C., (1998). "An experimental study of the influence of plate end anchorage of carbon fibre composite plates used to strengthen reinforced concrete beams." *Composite Structures.* 42, 175-188.

Garden, H. N., Hollaway, L. C., Thorne, A. M., (1997). "A preliminary evaluation of carbon fibre reinforced polymer plates for strengthening reinforced concrete members." *Proceedings of the Institution of Civil Engineers: Structures and buildings*. 123, 127-142.

Hussain, M., Sharif, A., Basunbul, I. A., Baluch, M. H. and Al- Sulaimani, G. J., (1995). "Flexural behaviour of precracked reinforced concrete beams strengthened externally by steel plates." *ACI Struct. J.*, 92(1), 14-22.

Jiang, D. S., Shah, P. and Andonian, A., (1984). "Study of the transfer of tensile forces by bond." *ACI Structural Journal*, 81(3), 251-259.

Jones, R., Swamy, R. N. and Ang, T. H., (1982). "Under- and overreinforced concrete beams with glued steel plates." *Int. J. Cem. Compos. Lightw. Concr.,* 4(1), 19-32.

Jones, R., Swamy, R. N. and Charif, A., (1988). "Plate separation and anchorage of reinforced concrete beams strengthened by epoxy-bonded steel plates." *Struct. Eng*., 66(5), 85-94.

JSCE, (2007). "Standard Specification for Concrete Structures - 2007: Design." Japan Society of Civil Engineers Tokyo: Japan.

Kankam, C., (1997). "Relationship of bond stress, steel stress, and slip in reinforced concrete." *Journal of Structural Engineering, ASCE,* 123(1), 79-85, 1997.

Maalej, M. and Bian, Y., (2001). "Interfacial shear stress concentration in FRP strengthened beams." *Composite Structures,* 54, 417-426.

Macdonald, M. D. and Calder, A. J. J., (1982). "Bonded steel plating for strengthening concrete structures." *International Journal of Adhesion and Adhesive*, 2(2),119-127.

Nguyen, D. M., Chan, T. K., Cheong. H. K., (2001). "Brittle failure and bond development length of CFRP Concrete Beams." *Journal of Composites for Construction,* 5(1), 12-17.

Oehlers, D. J., (1992). "Reinforced concrete beams with plates glued to their soffits." *J. Struct. Eng*., 118(8), 2023-2038.

Oller, I. E., Cobo del A. D. and Mari, B. A. R., (2009). "Peeling failure in beams strengthened by plate bond. A design proposal." *Journal of Structural concrete, fib ,* 2009,10, No2, 63-71.

Quantrill, R. J., Hollaway, L. C. and Thorne, A. M., (1996a). "Experimental and analytical investigation of FRP strengthened beam response: Part I." *Magazine of Concrete Research*. 48(177), 331-342.

Quantrill, R. J., Hollaway, L. C. and Thorne, A. M., (1996b). "Predictions of the maximum plate end stresses of FRP strengthened beams: Part II." *Magazine of Concrete Research*. 48(177), 343-351.

Rahimi, H. and Hutchinson, A., (2001). "Concrete beams strengthened with externally bonded FRP plates." *Journal of Composites for Construction*, 5(1), 44-56.

Raoof, M. and Hassanen, M. A. H., (2000). "Peeling failure of reinforced concrete beams with fibre-reinforced plastic or steel plates glued to their soffits." *Proceedings of the Institution of Civil Engineers: Structures and Buildings,* 14, 291-305.

Satoh, K. and Kodama, K., (2005) "Central peeling failure behavior of Polymer Cement Mortar Retrofitting of Reinforced Concrete Beams." *J. Mater. in Civil Eng*., 17(2), 126-136.

Smith, S. T. and Teng, J. G., (2002). "FRP-strengthened RC beam. II: Assessment of debonding strength models." *Engineering Structures,* 24, 397-417.

Swamy, R. N., Jones, R. and Bloxham, J. W., (1987). "Structural behavior of reinforced concrete beams strengthened by epoxy-bonded steel plate." *Struct. Eng.,* 65(2), 59-68.

Wu, Z. S., Yuan, H., Kojima, Y. and Ahmed, E., (2005). "Experimental and analytical studies on peeling and spalling resistance of unidirectional FRP sheets bonded to concrete." *Composites Science and Technology,* 65(7-8), 1088-1097.

Zhang, D. W., Ueda, T. and Furuuchi, H., (2011a). "Intermediate crack debonding of polymer cement mortar overlay-strengthened RC beam." *J. Mater. Civil Eng, ASCE,* 23(6):857-865.

Zhang, D. W., Ueda, T. and Furuuchi, H., (2011b). "Average crack spacing of overlay-strengthened RC beams." *J. Mater. Civil Eng, ASCE,* 23(10), 1460-1472.

Zhang, D. W., Furuuchi, H., Hori, A. and Ueda, T., (2009). "Fatigue degradation properties of PCM-concrete interface." *J. Adv. Concr. Technol.,* 7(3), 425-438.

Zhang, D. W., Ueda, T. and Furuuchi, H., (2012). "Concrete cover separation failure of overlay-strengthened reinforced concrete beams." *Construction and Building Materials,* 26(1), 735-745.

Zhang, S., Raoof, M. and Wood, L. A., (1995). "Prediction of peeling failure of reinforced concrete beams with externally bonded steel plates." *Proceedings of the Institution of Civil Engineers: Structures and Buildings,* 110, 257-268.

Appendix A: Experimental database for FRP laminate strengthened RC beam

Ref.	Name	b	h	a	d_0	A_{rc}	d_{rc}	A_r	d_r	$E_r=E_{rc}$	$f_{yr}=f_{yrc}$	t_s	b_s	A_s	E_s	f_{ys}	d_s	f'_c	f_{ct}	E_c
		mm	mm	mm	mm	mm^2	mm	mm^2	mm	MPa	MPa	mm	mm	mm^2	MPa	MPa	mm	MPa	MPa	MPa
Gao et al.	*Ga1*	150	200	500	150	50.27	27	78.54	162	2.00E+05	531	0.44	75	33	2.35E+05	4200	200.2	43.1	3.50	3.10E+04
	Gb1	150	200	500	150	50.27	27	78.54	162	2.00E+05	531	0.44	150	66	2.35E+05	4200	200.2	30	2.90	2.50E+04
	Gb2	150	200	500	150	50.27	27	78.54	162	2.00E+05	531	0.66	150	99	2.35E+05	4200	200.3	30	2.90	2.50E+04
Maalej and Bian	*MB3*	115	150	500	75	78.54	25	78.54	125	1.84E+05	534	0.222	115	25.53	2.30E+05	3400	150.1	30.3	2.90	2.60E+04
	MB4	115	150	500	75	78.54	25	78.54	125	1.84E+05	534	0.333	115	38.3	2.30E+05	3400	150.2	30.3	2.90	2.60E+04
	MB5	115	150	500	75	78.54	25	78.54	125	1.84E+05	534	0.444	115	51.06	2.30E+05	3400	150.2	30.3	2.90	2.60E+04
Rahimi and Hutchinson	*A4*	200	150	750	85	50.27	30	78.54	120	2.10E+05	350	0.8	150	120	1.27E+05	1532	150.4	50	3.00	2.50E+04
	A5	200	150	750	85	50.27	30	78.54	120	2.10E+05	350	0.8	150	120	1.27E+05	1532	150.4	50	3.00	2.50E+04
	B5	200	150	750	85	50.27	30	78.54	120	2.10E+05	350	1.2	150	180	1.27E+05	1532	150.6	50	3.00	2.50E+04
	B6	200	150	750	85	50.27	30	78.54	120	2.10E+05	350	1.2	150	180	1.27E+05	1532	150.6	50	3.00	2.50E+04
Fanning and Kelly	*FKF5*	155	240	1100	385	113.10	37	113.10	203	2.04E+05	532	1.2	120	144	1.55E+05	2400	240.6	80	4.27	3.92E+04
	FKF6	155	240	1100	385	113.10	37	113.10	203	2.04E+05	532	1.2	120	144	1.55E+05	2400	240.6	80	4.27	3.92E+04
	FKF7	155	240	1100	462	113.10	37	113.10	203	2.04E+05	532	1.2	120	144	1.55E+05	2400	240.6	80	4.27	3.92E+04
	FKF10	155	240	1100	550	113.10	37	113.10	203	2.04E+05	532	1.2	120	144	1.55E+05	2400	240.6	80	4.27	3.92E+04
Quantrill et al.	*B2*	100	100	300	20	28.27	15	28.27	85	2.15E+05	350	1.2	80	96	4.90E+04	2400	100.6	45.1	2.91	3.20E+04
	B4	100	100	300	20	28.27	15	28.27	85	2.15E+05	350	1.6	60	96	4.90E+04	2400	100.8	45.1	2.91	3.20E+04
Quantrill et al.	*A1c*	100	100	300	20	28.27	15	28.27	85	2.10E+05	350	1.2	80	96	4.90E+04	2400	100.6	59.5	3.51	3.65E+04
	A2b	100	100	300	20	28.27	15	28.27	85	2.10E+05	350	1.2	80	96	4.90E+04	2400	100.6	35.7	2.49	2.83E+04
	A2c	100	100	300	20	28.27	15	28.27	85	2.10E+05	350	1.2	80	96	4.90E+04	2400	100.6	35.7	2.49	2.83E+04
Garden and Hollaway	*1U,1.0m*	100	100	300	20	28.27	16	28.27	84	2.15E+05	350	0.82	67	54.94	1.11E+05	1370	100.4	45.9	2.95	3.20E+04
	2U,1.0m	100	100	300	20	28.27	16	28.27	84	2.15E+05	350	0.82	67	54.94	1.11E+05	1370	100.4	45.9	2.95	3.20E+04
Garden et al.	*1Au*	100	100	300	20	28.27	16	28.27	84	2.15E+05	350	0.5	90	45	1.11E+05	1273	100.3	50.2	3.13	3.35E+04
	1Bu	100	100	300	20	28.27	16	28.27	84	2.15E+05	350	0.7	65	45.5	1.11E+05	1273	100.4	50.2	3.13	3.35E+04
	1Cu	100	100	300	20	28.27	16	28.27	84	2.15E+05	350	1	45	45	1.11E+05	1273	100.5	50.2	3.13	3.35E+04
	2Au	100	100	340	20	28.27	16	28.27	84	2.15E+05	350	0.5	90	45	1.11E+05	1273	100.3	50.2	3.13	3.35E+04
	2Bu	100	100	340	20	28.27	16	28.27	84	2.15E+05	350	0.7	65	45.5	1.11E+05	1273	100.4	50.2	3.13	3.35E+04
	2Cu	100	100	340	20	28.27	16	28.27	84	2.15E+05	350	1	45	45	1.11E+05	1273	100.5	50.2	3.13	3.35E+04
	3Au	100	100	400	20	28.27	16	28.27	84	2.15E+05	350	0.5	90	45	1.11E+05	1273	100.3	50.2	3.13	3.35E+04

Appendix A: Experimental database for FRP laminate strengthened RC beam

Ref.	Name	b	h	a	d_0	A_{rc}	d_{rc}	A_r	d_r	$E_r=E_{rc}$	$f_{yr}=f_{yrc}$	t_s	b_s	A_s	E_s	f_{ys}	d_s	f'_c	f_{ct}	E_c
		mm	mm	mm	mm	mm^2	mm	mm^2	mm	MPa	MPa	mm	mm	mm^2	MPa	MPa	mm	MPa	MPa	MPa
Arduini et al.	*A3*	200	200	700	150	153.94	37	153.94	163	2.00E+05	540	1.3	150	195	1.67E+05	2906	200.7	33	2.37	2.50E+04
	A4	200	200	700	150	153.94	37	153.94	163	2.00E+05	540	1.3	150	195	1.67E+05	2906	200.7	33	2.37	2.50E+04
Nguyen et al.	*A950*	120	150	440	190	28.27	28	78.54	120	2.00E+05	384	1.2	80	96	1.81E+05	3400	150.6	27.3	2.09	2.50E+04
	A1100	120	150	440	115	28.27	28	78.54	120	2.00E+05	384	1.2	80	96	1.81E+05	3400	150.6	27.3	2.09	2.50E+04
	A1150	120	150	440	90	28.27	28	78.54	120	2.00E+05	384	1.2	80	96	1.81E+05	3400	150.6	27.3	2.09	2.50E+04
	NB2	120	150	440	115	28.27	23	314.16	120	2.00E+05	384	1.2	80	96	1.81E+05	3400	150.6	37.9	2.60	2.91E+04
Gao et al.	*1T6LN*	150	200	500	20	50.27	27	78.54	162	2.00E+05	531	0.66	150	99	2.35E+05	3400	200.3	47.8	3.03	3.25E+04
	2T6LN	150	200	500	20	50.27	27	78.54	162	2.00E+05	531	0.66	150	99	2.35E+05	3400	200.3	62.1	3.61	3.71E+04
	2T6L1a	150	200	500	20	50.27	27	78.54	162	2.00E+05	531	0.66	150	99	2.35E+05	3400	200.3	62.1	3.61	3.71E+04
	2T4LN	150	200	500	20	50.27	27	78.54	162	2.00E+05	531	0.44	150	66	2.35E+05	3400	200.2	62.1	3.61	3.71E+04
	2T4L1a	150	200	500	20	50.27	27	78.54	162	2.00E+05	531	0.44	150	66	2.35E+05	3400	200.2	62.1	3.61	3.71E+04
Ahmed and Gemert	*DF3*	125	225	500	50	28.27	32	50.27	193	1.85E+05	568	0.501	75	37.58	2.40E+05	3400	225.3	46	2.95	3.00E+04
	DF4	125	225	500	50	28.27	32	50.27	193	1.85E+05	568	0.668	75	50.1	2.40E+05	3400	225.3	46	2.95	3.00E+04
	AF3	125	225	500	100	28.27	32	50.27	193	1.85E+05	568	0.334	75	25.05	2.40E+05	3400	225.2	46	2.95	3.00E+04
Beber et al.	*VR5*	120	250	783	75	28.27	34	78.54	214	2.00E+05	565	0.44	120	52.8	2.30E+05	3400	250.2	33.6	3.10	2.74E+04
	VR6	120	250	783	75	28.27	34	78.54	214	2.00E+05	565	0.44	120	52.8	2.30E+05	3400	250.2	33.6	3.10	2.74E+04
	VR7	120	250	783	75	28.27	34	78.54	214	2.00E+05	565	0.77	120	92.4	2.30E+05	3400	250.4	33.6	3.10	2.74E+04
	VR8	120	250	783	75	28.27	34	78.54	214	2.00E+05	565	0.77	120	92.4	2.30E+05	3400	250.4	33.6	3.10	2.74E+04
	VR9	120	250	783	75	28.27	34	78.54	214	2.00E+05	565	1.1	120	132	2.30E+05	3400	250.6	33.6	3.10	2.74E+04
	VR10	120	250	783	75	28.27	34	78.54	214	2.00E+05	565	1.1	120	132	2.30E+05	3400	250.6	33.6	3.10	2.74E+04
Ahmed and Gemert	*CF2-1*	125	225	500	100	28.27	32	50.27	193	1.85E+05	568	0.334	75	25.05	2.40E+05	3400	225.2	46	2.95	3.00E+04
	CF4-1	125	225	500	100	28.27	32	78.54	193	1.85E+05	586	0.334	75	25.05	2.40E+05	3400	225.2	46	2.95	3.00E+04

Appendix B: Experimental database for steel plate strengthened RC beam

Ref.	Name	b	h	a	d_0	A_{rc}	d_{rc}	A_r	d_r	$E_r=E_{rc}$	f_{yr}	t_s	b_s	A_s	E_s	f_{ys}	d_s	f'_c	f_{ct}	E_c
		mm	mm	mm	mm	mm^2	mm	mm^2	mm	MPa	MPa	mm	mm	mm^2	MPa	MPa	mm	MPa	MPa	MPa
Hussain et al.	FRB2	150	150	400	50	28.27	30	78.54	120	2.00E+05	414	1	100	100	2.00E+05	269	150.5	31	2.27	2.63E+04
	FRB3	150	150	400	50	28.27	30	78.54	120	2.00E+05	414	1.5	100	150	2.00E+05	269	150.8	31	2.27	2.63E+04
	FRB5	150	150	400	50	28.27	30	78.54	120	2.00E+05	414	2	100	200	2.00E+05	269	151	31	2.27	2.63E+04
	FRB7	150	150	400	50	28.27	30	78.54	120	2.00E+05	414	3	100	300	2.00E+05	269	151.5	31	2.27	2.63E+04
Jones et al.	URB2	100	150	750	50	50.27	15	78.54	135	2.00E+05	530	1.5	80	120	2.00E+05	217	150.8	52.6	3.23	3.43E+04
	URB3	100	150	750	50	50.27	15	78.54	135	2.00E+05	530	3	80	240	2.00E+05	263	151.5	52.6	3.23	3.43E+04
	URB4	100	150	750	50	50.27	15	78.54	135	2.00E+05	530	5	80	400	2.00E+05	218	152.5	50.6	3.15	3.36E+04
	URB5	100	150	750	50	50.27	15	78.54	135	2.00E+05	530	10	80	800	2.00E+05	240	155	52.6	3.23	3.43E+04
Oehlers	I/2/S	130	175	550	100	78.54	30	201.06	147	2.00E+05	444	5	130	650	2.00E+05	272	177.5	42	2.78	2.20E+04
	I/2/N	130	175	550	150	78.54	30	201.06	147	2.00E+05	444	5	130	650	2.00E+05	272	177.5	42	2.78	2.20E+04
	I/3/S	130	175	550	250	78.54	30	201.06	147	2.00E+05	444	5	130	650	2.00E+05	272	177.5	42	2.78	2.20E+04
	I/3/N	130	175	550	400	78.54	30	201.06	147	2.00E+05	444	5	130	650	2.00E+05	272	177.5	42	2.78	2.20E+04
	I/4/S	130	175	550	50	78.54	30	201.06	147	2.00E+05	444	5	130	650	2.00E+05	272	177.5	42	2.78	2.20E+04
	2/1/N	130	175	550	300	78.54	30	201.06	147	2.00E+05	444	5	130	650	2.00E+05	272	177.5	47	3.00	2.90E+04
	2/1/S	130	175	550	75	78.54	30	201.06	147	2.00E+05	444	5	130	650	2.00E+05	272	177.5	47	3.00	2.90E+04
	2/2/N	130	175	550	300	78.54	30	201.06	147	2.00E+05	444	5	130	650	2.00E+05	272	177.5	47	3.00	2.90E+04
	2/2/S	130	175	550	75	78.54	30	201.06	147	2.00E+05	444	5	130	650	2.00E+05	272	177.5	47	3.00	2.90E+04
	2/3/N	130	175	550	300	78.54	30	201.06	147	2.00E+05	444	5	130	650	2.00E+05	272	177.5	47	3.00	2.90E+04
	2/3/S	130	175	550	75	78.54	30	201.06	147	2.00E+05	444	5	130	650	2.00E+05	272	177.5	47	3.00	2.90E+04
	2/4/N	130	175	550	300	78.54	30	201.06	147	2.00E+05	444	5	130	650	2.00E+05	272	177.5	47	3.00	2.90E+04
	2/4/S	130	175	550	75	78.54	30	201.06	147	2.00E+05	444	5	130	650	2.00E+05	272	177.5	47	3.00	2.90E+04
	5/1/N	130	175	550	400	78.54	30	201.06	147	2.00E+05	444	5	130	650	2.00E+05	272	177.5	49	3.08	2.90E+04
	5/1/S	130	175	550	150	78.54	30	201.06	147	2.00E+05	444	5	130	650	2.00E+05	272	177.5	49	3.08	2.90E+04
	6/1/-	130	175	925	625	78.54	30	201.06	147	2.00E+05	444	5	130	650	2.00E+05	272	177.5	52	3.20	3.00E+04
	6/2/-	130	175	925	625	78.54	30	201.06	147	2.00E+05	444	5	130	650	2.00E+05	272	177.5	52	3.20	3.00E+04
	6/3/-	130	175	1125	825	78.54	30	201.06	147	2.00E+05	444	5	130	650	2.00E+05	272	177.5	52	3.20	3.00E+04
	6/4/-	130	175	1225	825	78.54	30	201.06	147	2.00E+05	444	5	130	650	2.00E+05	272	177.5	52	3.20	3.00E+04
	7/1/S	130	175	1400	1000	78.54	30	201.06	147	2.00E+05	444	5	130	650	2.00E+05	272	177.5	51	3.16	3.20E+04
	8/2/S	130	175	1700	1300	78.54	30	201.06	147	2.00E+05	444	5	130	650	2.00E+05	272	177.5	40	2.69	2.70E+04
Swamy et al.	204	155	255	767	50	28.27	30	314.16	220	2.00E+05	470	3	125	375	2.00E+05	258	258	53.12	3.25	3.60E+04
	205	155	255	767	50	28.27	30	314.16	220	2.00E+05	470	6	125	750	2.00E+05	248	259.5	56.16	3.37	3.60E+04
	208	155	255	767	50	28.27	30	314.16	220	2.00E+05	470	3	125	375	2.00E+05	258	259.5	54.4	3.30	3.60E+04
	209	155	255	767	50	28.27	30	314.16	220	2.00E+05	470	6	125	750	2.00E+05	248	261	57.76	3.44	3.60E+04
	210	155	255	767	50	28.27	30	314.16	220	2.00E+05	470	6	125	750	2.00E+05	248	261	56.24	3.38	3.60E+04
	216	155	255	767	50	28.27	30	314.16	220	2.00E+05	470	1.5	125	188	2.00E+05	236	261.8	54.72	3.32	3.60E+04
	217	155	255	767	50	28.27	30	314.16	220	2.00E+05	470	3	125	375	2.00E+05	258	262.5	54.88	3.32	3.60E+04
	218	155	255	767	50	28.27	30	314.16	220	2.00E+05	470	6	125	750	2.00E+05	248	264	57.2	3.41	3.60E+04
	219	155	255	767	50	28.27	30	314.16	220	2.00E+05	470	6	125	750	2.00E+05	248	264	58.4	3.46	3.60E+04
	224	155	255	767	50	28.27	30	314.16	220	2.00E+05	470	3	125	375	2.00E+05	258	259.5	56.88	3.40	3.60E+04